

Spatial assessment of the physiological status of wheat crops as affected by water and nitrogen supply using infrared thermal imagery

D. Rodriguez^{A,C}, V. O. Sadras^B, L. K. Christensen^A, and R. Belford^A

^ADepartment of Primary Industries, Primary Industries Research Victoria, PB 260, Horsham, Vic. 3401, Australia.

^BCSIRO–APSRU, PMB 2, Glen Osmond, SA 5064, Australia.

^CCorresponding author; present address: Agricultural Production Systems Research Unit, Department of Primary Industries and Fisheries, PO Box 102, Toowoomba, Qld 4350, Australia. Email: daniel.rodriguez@dpi.qld.gov.au

Abstract. This work addresses the need for meaningful spatial indices of the physiological condition of field crops for site-specific management and variable rate application in precision agriculture. Precision agriculture is designed to target crop inputs according to within-field requirements to increase profitability while protecting the environment. The objectives of this work were to (a) develop a canopy physiological stress index with spatial resolution commensurate with the needs of site-specific management, and (b) test the physiological meaning of this index by exploring its association with key processes and variables at leaf and crop levels. We report results from a single-year field experiment where different levels of irrigation, wheat crop density, and nitrogen supply were applied to increase the expression of within-season variability. We defined a canopy stress index (CSI) as the difference between canopy (T_c), and air temperature (T_a), normalised by vapour pressure deficit (VPD): $CSI = (T_c - T_a)/VPD$. A novel method to extract canopy temperatures (T_c) from complex digital thermal images was developed, thus allowing for the spatial characterisation of CSI. CSI is expected to be positive and high if the capacity of the canopy to dissipate heat is reduced as when stomata close. CSI accounted for 80% of the variation in growth rate and yield, compared with 46–49% explained by the normalised difference vegetation index (NDVI). Most of the variation in crop response variables was related to water supply. The physiological meaning of this index was reinforced by its significant association with gas exchange variables measured at the leaf-level. The potential for the use of digital thermal imaging in precision agriculture is discussed.

Additional keywords: precision agriculture, thermal digital imaging, stomatal conductance, photosynthesis, NDVI.

Introduction

The site-specific management of crops and variable rate technologies heavily rely on rapid, accurate, and affordable techniques to spatially monitor the physiological status of crops and their potential response to tactical interventions, such as in-season nitrogen application.

Multispectral and hyperspectral sensors have been widely used to assess spatial variation in crop phenology (Railyan and Korobov 1993), crop growth and yield (Price and Bausch 1995), concentration of pigments (Filella and Peñuelas 1994), and nutrients (Filella and Peñuelas 1994; Blackmer *et al.* 1996). Common assessment techniques are based on the absorption of light in the visible portion of the spectrum and reflection of near-infrared light by plant tissues. Although spectral screening has been used to quantify spatial and temporal variation in crop properties, e.g. nitrogen fertilisation (Stone *et al.* 1997), confounding factors such as

crop water stress (Moran *et al.* 1997) restrict their practical value. Water deficit is a trademark of rainfed cereal crops in Australia, where the potential for crop response to in-season tactical management of nitrogen heavily relies on available soil water and spring rainfall.

The physiological condition of crops has been previously quantified with infrared thermometry to develop point canopy water stress indices used for crop management and even cultivar screening (Idso 1982; Garrity and O'Toole 1995). This was based upon the assumption that, as water becomes limiting, transpiration is reduced and the plant temperature increases. The crop water stress index (CWSI) of Idso *et al.* (1981) and Jackson *et al.* (1981) was defined as the difference between crop temperature and air temperature, normalised by atmospheric conditions using the vapour pressure deficit. CWSI was used to predict soil moisture content (Jackson 1982) and

plant transpiration (Jackson *et al.* 1983). However, the difficulty of measuring foliage temperature from partially vegetated fields, with hand-held infrared thermometers, and most airborne and satellite-based infrared sensors, limited its application. Before a crop achieves full cover the temperature of the soil generally dominates the composite, i.e. soil–crop, temperature measurements. Moran *et al.* (1994) expanded the CWSI concept by combining spectral vegetation indices with surface temperatures to allow the application of the CWSI theory to partially vegetated fields when the temperature of the crop is unknown. The resulting water deficiency index (WDI) had potential for evaluating evapotranspiration rate and relative field water deficit for both full-cover and partially vegetated sites. Recent advances and availability of equipment for digital thermal imaging provide a unique opportunity to develop instantaneous spatial canopy stress indices for use in precision agriculture (Chaerle and van der Straten 2000). In this work, we hypothesise that (i) an index simply based on the difference between the canopy and air temperatures, normalised by vapour pressure deficit, can be used to spatially identify areas in the field undergoing contrasting levels of water stress, and (ii) canopy temperature can be retrieved from complex thermal images of mixed soil–canopy pixels by using vegetative indices of ground cover. The objectives of this work were to (a) develop a simple canopy physiological stress index with spatial resolution commensurate with the needs of site-specific management, and (b) test the physiological meaning of this index by exploring its association with key processes and variables at leaf and canopy levels.

Materials and methods

Crops, treatments, and experimental design

A field experiment was set up in Horsham (36.65°S, 142.10°W) on a Grey Vertosol. At sowing, soil nitrogen was 180 kg N/ha (0–1 m), soil phosphorus 30 mg/kg (0–0.2 m), and soil pH_{H₂O} 8.8 (0–1 m). Wheat (*Triticum aestivum* L., cv. Chara) was sown on the 17 June 2004. At sowing a triple super phosphate fertiliser (46% P₂O₅) was applied to all the experimental plots at a rate of 61 kg fertiliser/ha. The crop emerged 9 days after sowing. Two plant densities (52 and 102 kg seed/ha), 4 rates of nitrogen fertiliser (0, 16, 39, and 163 kg N/ha) applied as urea (46% N), and 2 water regimes (irrigated and rainfed) were combined in a factorial experiment with 3 replicates. Treatments were arranged in a split-plot design where the nitrogen and density levels were randomised to subplots within the irrigation main plots. The irrigated plots were watered using an automatic sprinkler system every time the accumulated rainfall deficit reached 20–50 mm, with respect to a decile 9 of rainfall in Horsham. At maturity, in-crop rainfall, i.e. 22 June–20 December, totalled 270 mm, and an additional 120 mm were applied to the irrigated treatments, corresponding with deciles 5 and 9 at Horsham, respectively. Weeds, pests, and diseases were frequently monitored and controlled as required. An additional ‘control plot’ of 9 m², set up outside the main experimental field, was sown with the high plant density, i.e. 102 kg seed/ha, fertilised with 163 kg N/ha, and frequently irrigated shortly before gas exchange measurements.

Crop, soil, and weather measurements

Shoots were sampled at about fortnightly intervals to determine dry weights of whole shoot and its components (laminae, stem + sheath, and ears). Photosynthetically active radiation (PAR) intercepted by the canopy was determined at each sampling time using a ceptometer (CropScan, Delta-T Devices Ltd, Cambridge, UK). At anthesis, the rate of gas exchange of flag leaves, and related variables, were determined in the high plant density treatments, using a LiCor 6400 leaf gas exchange system (Li-Cor, Nebraska, USA). Solar radiation, temperature, wind speed, and relative humidity were recorded at 20-min intervals in a weather station installed at the experimental site. Climatic records (103 years) for Horsham, i.e. Station 79023 (located at about 7 km from the experimental site), were obtained from the Australian Bureau of Meteorology.

Remote sensing of canopy properties

Canopy temperature at anthesis was used to calculate a canopy stress index as described below. Canopy temperature was measured using both a hand-held infrared thermometer (Everest 100.3ZL, Everest Interscience, Tucson, USA) and a ThermoCam P40 (Flir Systems AB, Danderyd, Sweden). Both instruments were calibrated against a black body (Everest Interscience, Tucson, USA). The infrared thermometer was held at an angle of 20–30 degrees to the horizontal and at a height to give a canopy viewing area of approximately 0.2 m by 0.5 m. Several readings were taken between 1300 and 1500 hours from the eastern side of north–south oriented plots. The ThermoCam P40 was used to measure canopy temperature from thermal images of 1-m² areas of the crop canopy taken from 2.5 m above ground level in a nadir direction. Simultaneous with these measurements, air temperature and relative humidity above the canopy were recorded with a Vaisala HM70 (Vaisala, Helsinki, Finland). In addition, on 10 October, the ThermoCam P40 was flown in an aircraft at 600 m above the experimental site, and thermal images were acquired in a nadir direction at noon. The images were processed using ThermoCam Researcher Pro 2.8 SR-1 (Flir Systems AB, Danderyd, Sweden) and exported into MatLab 7.0.1 (The MathWorks Inc., Natick, USA) for numerical analysis and image processing.

At anthesis, crop reflectance in the red and near-infrared ranges was measured using an active sensor, i.e. not limited by ambient lighting conditions (Crop Circle ACS-210, Holland Scientific, Nebraska, USA). The sensor was located 1 m above the canopy and averages of 20 readings over 2 lineal metres of crop were recorded. From reflectance readings, we derived the normalised difference vegetation index (NDVI; Rouse *et al.* 1973), the ratio vegetation index (RVI; Jordan 1979), and the soil adjusted vegetation index (SAVI; Huete 1988).

Canopy stress index (CSI)

Based on the work of Idso *et al.* (1981) and Idso (1982), we defined a canopy stress index (CSI) as the difference between canopy (T_c) and air temperature (T_a), normalised by vapour pressure deficit (VPD):

$$CSI = (T_c - T_a)/VPD \text{ (}^\circ\text{C/kPa)} \quad (1)$$

CSI is expected to be positive and high if the capacity of the canopy to dissipate heat is reduced, as when stomata close. A range of environmental factors could cause stomatal closure, including drought (Jones *et al.* 1995), and pests and diseases affecting vascular tissue, roots, or foliage (Boccaro *et al.* 2001; Chaerle *et al.* 1999; Bowden *et al.* 1990; Sadras and Wilson 1997). Stomatal closure can also be induced by shortage of nutrients (Radin *et al.* 1985; Broadley *et al.* 2001), and by hormonal signals (Bringham 2001). Consequently, CSI is an index of the general physiological status of a canopy.

The spatial variation in CSI across a field can be derived from thermal images of small areas of the canopy or from images of entire fields, where the field of view receives the emittance from canopies and soil (Fig. 1). For the spatial derivation of the canopy stress index (Eqn 1), methods are required to retrieve canopy temperature (T_c) from spatially variable combinations of canopy and soil. Quantitatively, the average temperature of an image (T_i) depends on the fraction of soil and canopy captured in the image, and on the actual canopy and soil temperature. Theoretically, canopy temperature and T_i converge as canopy size approaches full ground cover (Fig. 2a). Hence, canopy temperature could be calculated as:

$$T_c = T_i - \Delta \text{ (}^\circ\text{C)} \quad (2)$$

where Δ is the difference between the estimated average temperature of the image and the actual temperature of the crop. This variable is expected to be an inverse function of ground cover (GC):

$$\Delta = f(\text{GC}^{-1}) \text{ (}^\circ\text{C)} \quad (3)$$

The hypothetical relationship in Eqn 2 and Fig. 2a was tested using thermal images, where T_i is the average for the whole image, and T_c is measured in sections of the image unequivocally identified as ‘canopy’. The relationship in Eqn 3 was tested using both point measures of canopy ground cover assessed as fractional PAR interception ($1 - f$), and vegetation indices derived from the readings with the Crop Circle sensor.

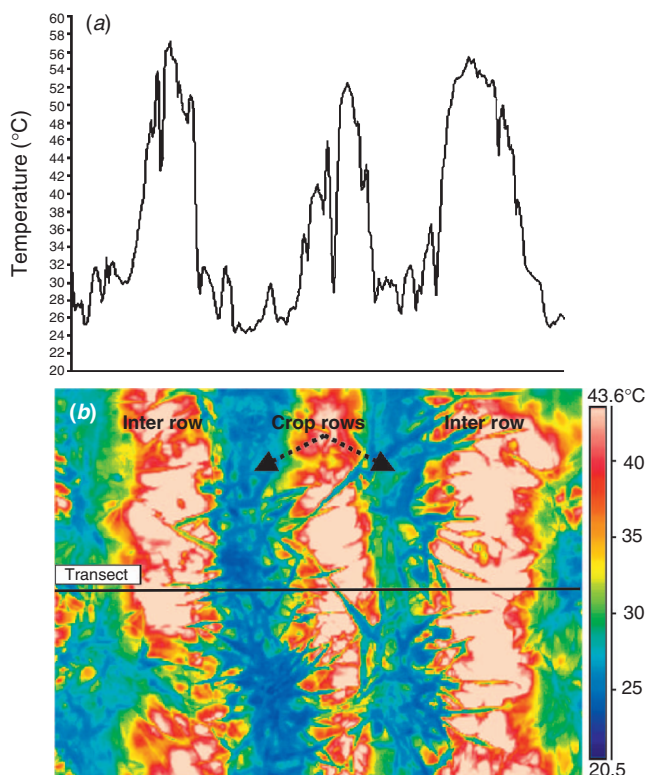


Fig. 1. (a) Profile of crop and soil temperatures derived from (b) a digital thermal image of a wheat canopy taken at 3 m above ground level at Decimal Code (DC) 31.

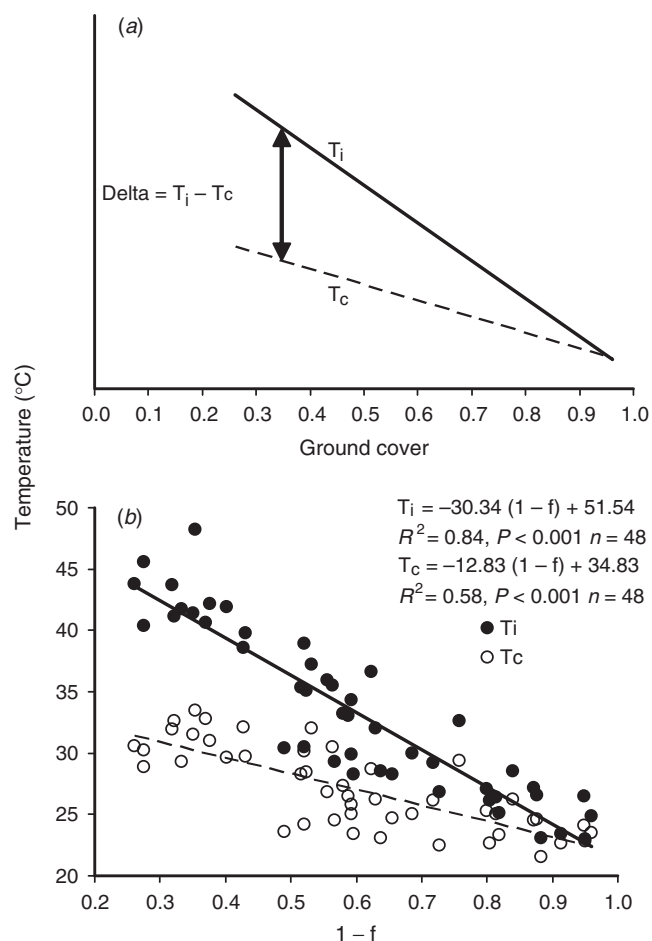


Fig. 2. (a) Hypothetical and (b) actual convergence of canopy (T_c , open symbols) and average image temperature (T_i , closed symbols) as a function of ground cover. In (b), $1 - f$ is the fractional PAR interception.

Results

Seasonal conditions

Figure 3 summarises meteorological conditions during the experiment. The main feature of the cropping season was a long dry spell around anthesis. Rainfall plus irrigation from emergence to harvest amounted to 270 and 390 mm in the rainfed and irrigated treatments, respectively. These values corresponded to long-term deciles 5 and 9 at Horsham (SILO Station 79023). Extreme temperatures further contributed to the stressful conditions during the most critical period for grain yield determination (Fischer 1985; Loomis and Connor 1996). On 16 October (closed diamond in Fig. 3b), temperature was below zero for a period of about 4 h from 0240 hours. On 12 October (open diamond in Fig. 3b), temperature was above 31°C from 1140 until 1900 hours, and peaked at 37°C; average daily vapour pressure deficit was 1.5 kPa, with an absolute maximum of 6 kPa at 1600 hours.

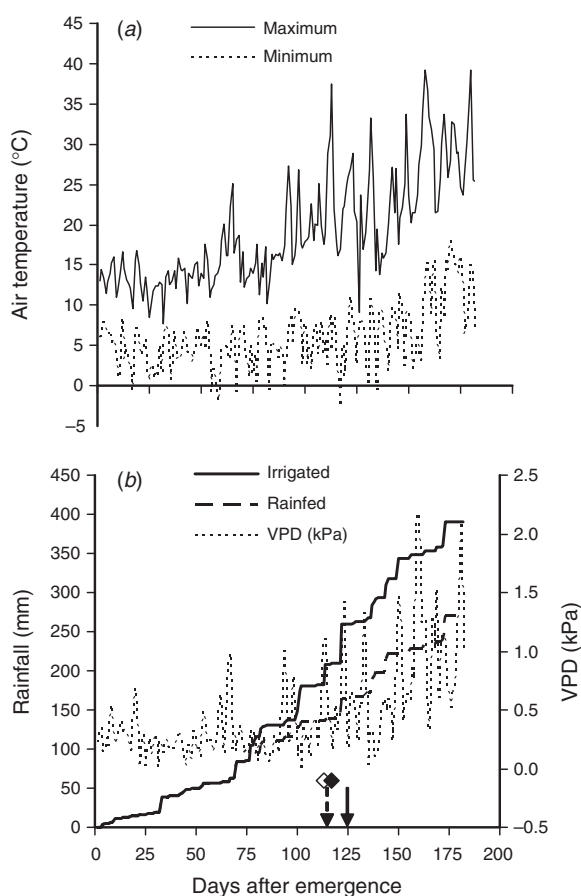


Fig. 3. (a) Seasonal course of maximum and minimum temperatures, and (b) cumulative rainfall + irrigation, and vapour pressure deficit. Vapour pressure deficit was derived from dry- and wet-bulb temperatures at 0900 hours. The arrows indicate the date of anthesis for the irrigated and rainfed plots. The diamonds indicate occurrence of extreme high (open), and low (closed) temperatures events, respectively.

Crop development, growth, and yield

Anthesis (Decimal Code 61) started at 115 days after emergence (DAE) for all the rainfed plots and irrigated low-nitrogen treatments, and at 121 DAE for the irrigated, high-nitrogen plots (Fig. 3b).

Water supply was the main source of variation in shoot growth rate prior to anthesis ($P = 0.062$), which varied from -4.5 to $16.5 \text{ g/m}^2\cdot\text{day}$ (Table 1). Both water and nitrogen supply affected grain yield (Table 2). Compared with the rainfed plots, average grain yields were 3 times higher in the irrigated plots, and were highest for the intermediate rates of nitrogen.

Ear tipping, damage of the ear by drought and heat stress (Fischer and Wood 1979), was only observed in the rainfed plots and was more severe for the normal plant density and highest nitrogen rate (Table 3). Ear tipping explained only 23% ($P = 0.23$, $n = 8$) of the variation in grain yield of rainfed plots.

Table 1. Rate of growth ($\text{g/m}^2\cdot\text{day}$) between 12 days before anthesis and anthesis of a wheat crop growing under 2 levels of irrigation, 2 plant densities, and 4 nitrogen rates (kg N/ha)

The least significant difference of means (5% level) for the irrigation \times nitrogen \times density comparison is $13.9 \text{ g/m}^2\cdot\text{day}$

N rate	Rainfed		Irrigated	
	Half density	Normal density	Half density	Normal density
0	0.0	3.0	16.5	11.0
16	-0.1	1.5	12.0	11.6
39	-4.5	8.8	12.6	11.2
163	0.7	2.0	10.1	10.9

Table 2. Grain yield (kg/ha) of wheat crops growing under 2 levels of irrigation, 2 plant densities, and 4 nitrogen rates (kg N/ha)

The least significant difference of means (5% level) for the irrigation \times nitrogen \times density comparison is 1556 kg/ha

N rate	Rainfed		Irrigated	
	Half density	Normal density	Half density	Normal density
0	1245	1341	4181	3361
16	1446	1537	4505	4862
39	2043	1845	3889	4767
163	1005	525	3200	4174

Table 3. Ear tipping (%) 2 weeks after anthesis of wheat crops growing under 2 levels of irrigation, 2 plant densities, and 4 nitrogen rates (kg N/ha)

The least significant difference of means (5% level) for the irrigation \times nitrogen \times density comparison is 24.8%

N rate	Rainfed		Irrigated	
	Half density	Normal density	Half density	Normal density
0	10.0	21.7	0.0	0.0
16	20.0	28.3	0.0	0.0
39	26.7	36.7	0.0	0.0
163	33.3	60.0	0.0	0.0

Relationship between canopy and whole image temperature

The proposed convergence of canopy and whole-image temperature with increasing canopy cover (Fig. 2a) was verified in crops where canopy cover and its actual physiological condition were affected by the supply of water, nitrogen, and plant population density (Fig. 2b).

All 3 tested vegetation indices proved reasonable estimators of the gap (*Delta*) between canopy and whole-image temperature and they all were related to fractional PAR interception, a direct indicator of ground cover (Fig. 4). Thus, the combination of thermal images and vegetation indices might provide the basis for retrieving canopy temperature from complex thermal images of canopy and soil, although

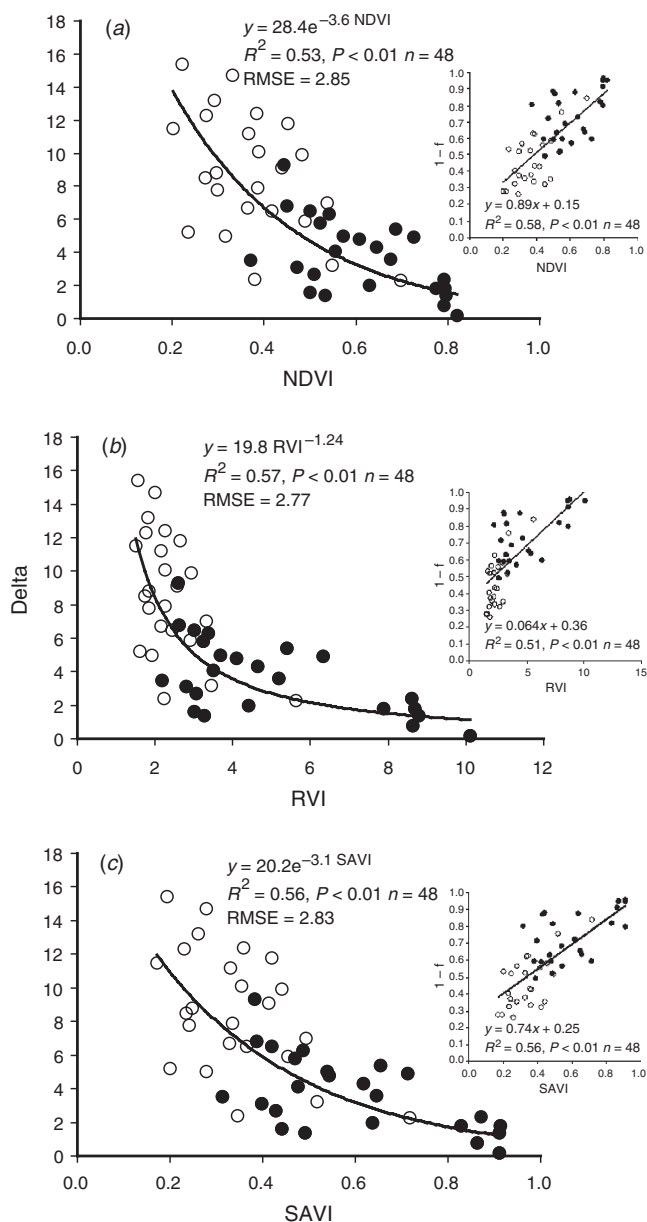


Fig. 4. Difference (*Delta*) between thermal-image average temperature (T_i) and canopy temperature (T_c) at anthesis of wheat as a function of (a) the normalised difference vegetation index (NDVI), (b) the ratio vegetation index (RVI), and (c) the soil adjusted vegetation index (SAVI) determined at anthesis. Insets show the relationship between the fractional intercepted radiation ($1 - f$) and the vegetation indices. Closed symbols are for irrigated plots and open symbols for rainfed plots.

the base lines in Fig. 2 can be expected to move as affected by micrometeorological conditions and by the top-soil water content, with smaller *Deltas* under wet soil conditions.

Effect of water and nitrogen supply on NDVI and CSI

The effect of water and nitrogen supply on the sensed indices and crop performance was studied at anthesis, a key

critical stage for final grain yield definition (Fischer 1985). Anthesis NDVI was significantly affected by both irrigation ($P = 0.024$) and nitrogen supply ($P < 0.001$), indicating that NDVI could be used to identify underperforming areas in the field (Table 4). However, NDVI alone cannot discriminate between nitrogen deficiency and water stress driven by dry subsoil, chemical constraints (Sadras *et al.* 2004; Rodriguez *et al.* 2005), or root pests and diseases (Bowden *et al.* 1990; Sadras and Wilson 1997). CSI was affected by water supply ($P = 0.005$) but not by nitrogen rate (Table 4), indicating that CSI could be used to represent the physiological condition of the canopy and its potential for response to remedial actions such as top dressing with nitrogen fertilisers (Clarke 1997; Barnes *et al.* 2000).

Leaf gas exchange and CSI

Stomatal conductance, net assimilation rate, and transpiration rate at anthesis were lower in the rainfed plots ($P < 0.001$). The highest stomatal conductance ($0.286 \text{ mol/m}^2.\text{s}$), net photosynthetic rate ($25.2 \text{ } \mu\text{mol CO}_2/\text{m}^2.\text{s}$), and transpiration rate ($3.9 \text{ } \mu\text{mol H}_2\text{O/m}^2.\text{s}$) were observed in a well-irrigated, high-nitrogen control plot located beside the experimental field that had a CSI of -1.04°C/kPa . At the leaf level, CSI explained 44, 63, and 36% of the variation in normalised stomatal conductance, net photosynthesis, and transpiration rate, respectively (Fig. 5).

Relationships between crop growth rate, yield, NDVI, and CSI

Shoot growth rate before anthesis explained 81% of the variation in grain yield (Fig. 6). Figures 7 and 8 summarise the relationships between NDVI and CSI at anthesis, and 2 crop response variables, i.e. shoot growth rate and yield.

Table 4. Normalised difference vegetative index (NDVI) and canopy stress index (CSI) at anthesis of wheat crops growing under 2 levels of irrigation, 2 plant densities, and 4 nitrogen rates (kg N/ha)

The least significant differences of means (5% level) for the irrigation \times nitrogen \times density comparison are 0.16 and 1.1°C/kPa for the NDVI and CSI, respectively

N rate	Rainfed		Irrigated	
	Half density	Normal density	Half density	Normal density
<i>NDVI</i>				
0	0.29	0.32	0.56	0.43
16	0.36	0.29	0.59	0.51
39	0.33	0.47	0.56	0.63
163	0.48	0.44	0.80	0.78
<i>Canopy stress index ($^\circ\text{C/kPa}$)</i>				
0	4.17	3.43	1.20	1.67
16	3.87	4.57	1.60	2.07
39	3.77	3.50	0.93	1.60
163	4.23	3.10	1.30	1.10

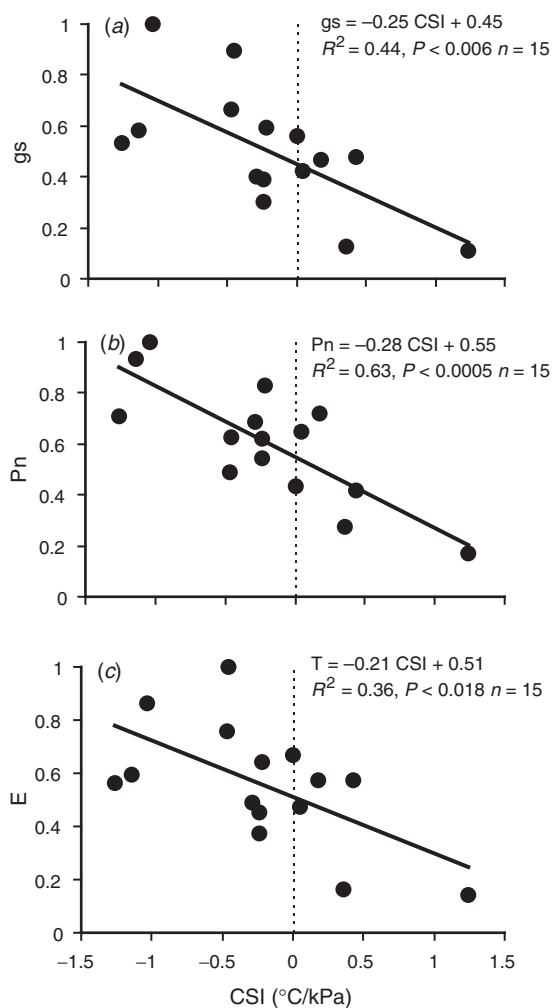


Fig. 5. Relationship between (a) leaf stomatal conductance, (b) leaf net photosynthesis rate, and (c) leaf transpiration rate, and the canopy stress index (CSI). Response variables are normalised relative to maxima measured in a well-irrigated, high-nitrogen control.

CSI accounted for 80% of the variation in growth rate and yield, compared with 49% and 46% for NDVI, respectively. Most of the variation in crop response variables was related to water supply.

Application of the CSI

As an example of the potential application of the CSI, we derived its value for each pixel of an airborne digital thermal image of the experimental site assuming a unique value of NDVI for each plot. The image was taken on 10 October 2004 at noon (air temperature = 27.2°C and VPD = 2.78 kPa). Figure 9 shows the spatial variation in CSI. In general, CSI was low and negative in the irrigated plots, and high and positive in the rainfed plots. The spatial variation was less in rainfed plots (s.e. = 0.34) than in their irrigated counterparts (s.e. = 0.56). The variation within the rainfed plots was most likely related to soil properties, whereas soil properties

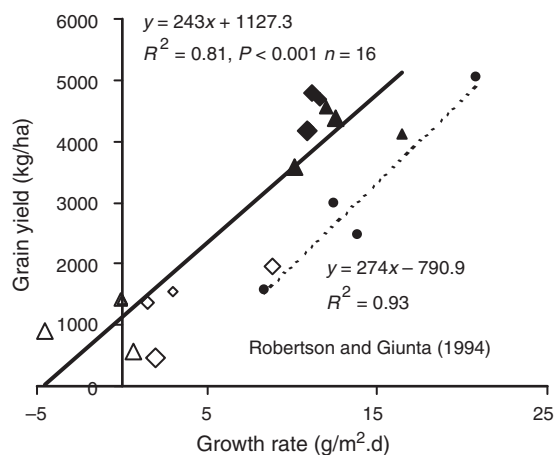


Fig. 6. Wheat grain yield (kg/ha) as a function of shoot growth rate prior to anthesis ($\text{g/m}^2\cdot\text{day}$), for irrigated (closed symbols) and rainfed (open symbols) plots, high (diamonds) and low (triangles) plant densities, and 4 nitrogen rates (0, 16, 39, and 163 kg N/ha) represented by the increasing size of the symbols. Every point is the average of 3 replications. The small circles and the dotted line are data points from Robertson and Giunta (1994).

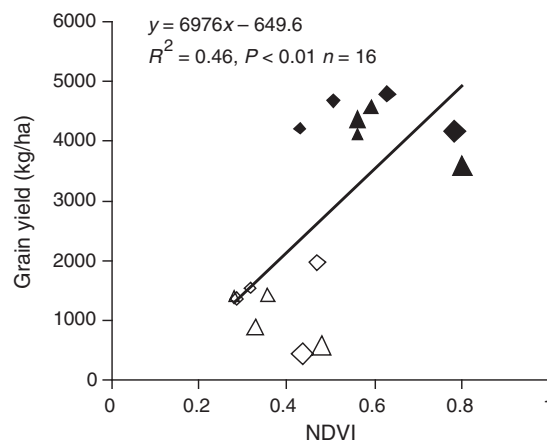


Fig. 7. Grain yield of wheat crops as function of the normalised difference vegetation index (NDVI). Symbols: irrigated (closed), rainfed (open); high (diamonds) and low (triangles) plant densities, and 4 nitrogen rates (0, 16, 39, and 163 kg N/ha) represented by the increasing size of the symbols. Every point is the average of 3 replications.

and border effects both contributed to the variation in irrigated plots.

Discussion

The detection of stress conditions in crops at field level requires indices to spatially rate the potential for profitable management interventions, such as top dressing with nitrogen on large areas of land. Visual assessments of crop condition can be effective when performed by an experienced farmer. However, by the time visual symptoms of stress are present, the crop has already been adversely

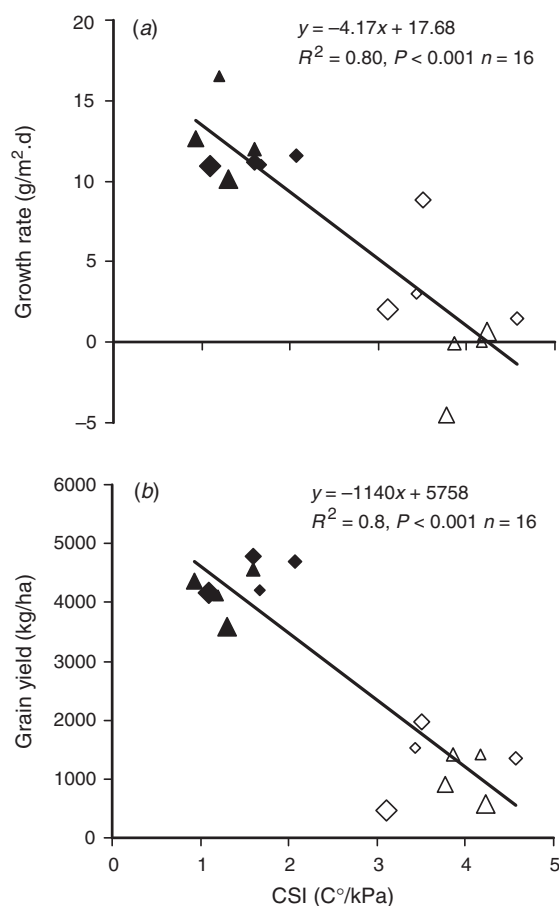


Fig. 8. (a) Wheat growth rate around anthesis (g/m².day) and (b) grain yield (kg/ha) as a function of the crop stress index (CSI, C°/kPa) calculated at anthesis, for the irrigated (closed symbols) and rainfed (open symbols) plots, high (diamonds) and low (triangles) plant densities, and 4 levels of nitrogen (0, 16, 39, and 163 kg N/ha) represented by the increasing size of the symbols. Every point is the average of 3 replications.

affected and remedial interventions may have little or no benefit. Present applications of pre-symptomatic detection of stressful conditions in the field are generally based on the differential capacity of green crops to strongly absorb red radiation and reflect near-infrared radiation. The ratio red/near-infrared has been long used to identify under-performing areas in large areas of crops (Peñuelas and Filella 1998), and to correct in-season nitrogen fertiliser deficiencies (Stone *et al.* 1997). However, the technique is limited as it is difficult to determine if the relationship between a spectral response and crop condition that alters canopy density, e.g. nitrogen or water stress, is truly a unique spectral signature or simply an artefact of changes in canopy density (Barnes *et al.* 2000). Furthermore, the spatial patterns in canopy density might not directly reflect changes in N supply and the potential for response to in-season additions of N, making the use of spectral indices from canopies

alone, unsuitable to be used in variable rate applications of N fertilisers. The combination of spectral and thermal properties of the canopy has been used to produce maps of water stress, N status, and canopy density, when variations in all of these factors were simultaneously present in the field (Barnes *et al.* 2000). Under Australian conditions, matching nitrogen supply to water availability is key to the success of wheat crops. Shortage of nitrogen can impair yield and reduce water use efficiency, and excess nitrogen, particularly early in the season, can reduce grain yield through the production of excessive biomass and the haying-off of the crop (van Herwaarden *et al.* 1998a, 1998b). Therefore, the development of spatial indices able to identify areas in the field of potentially positive response to management intervention such as top dressing with nitrogen fertilisers becomes paramount. The objectives of this work were to (a) develop a canopy physiological stress index with spatial resolution commensurate with the needs of site-specific management, and (b) test the physiological meaning of this index by exploring its association with key processes and variables at leaf and crop levels.

Based on the work of Idso *et al.* (1981), we developed an index of the physiological status of the crop that could be applied spatially over large areas in the field to assist in identifying areas having high and low potential for response to management intervention. In a second paper we will address the issue of the spatial identification of nitrogen stresses in wheat canopies growing under contrasting canopy densities and water status.

This work reports results from one growing season. To account for the effects of seasonal conditions, chiefly variation in rainfall, we established irrigation regimes corresponding to in-crop rainfall deciles 5 and 9. Although the rainfed treatment was in the average rainfall range (decile 5), seasonal distribution of rain, with a long dry spell around anthesis (Fig. 3), determined unfavourable conditions during the key period of grain set (Fischer 1985). Temperature stress around anthesis compounded the effect of water shortage (Fig. 3, Table 3). Hence, this study encompassed an important range of expected seasonal conditions for the Wimmera region of Victoria, Australia.

Despite the high nitrogen and irrigation treatment, growth rates around anthesis and grain yields were below the potential for the region. Most likely the dry conditions and extreme temperatures around anthesis were responsible for an important reduction in growth and yield potential in both irrigated and rainfed plots. Understanding crop responses to weather extremes is incomplete, although temperature above 31°C immediately before anthesis could cause pollen sterility and reduce grain yield (Wheeler *et al.* 1996). Sub- or super-optimal temperatures during anthesis may also reduce yield through the production of sterile florets (Russell and Wilson 1994). In Australia, Stone and Nicolas (1995) showed that plants are most sensitive to high temperatures during the

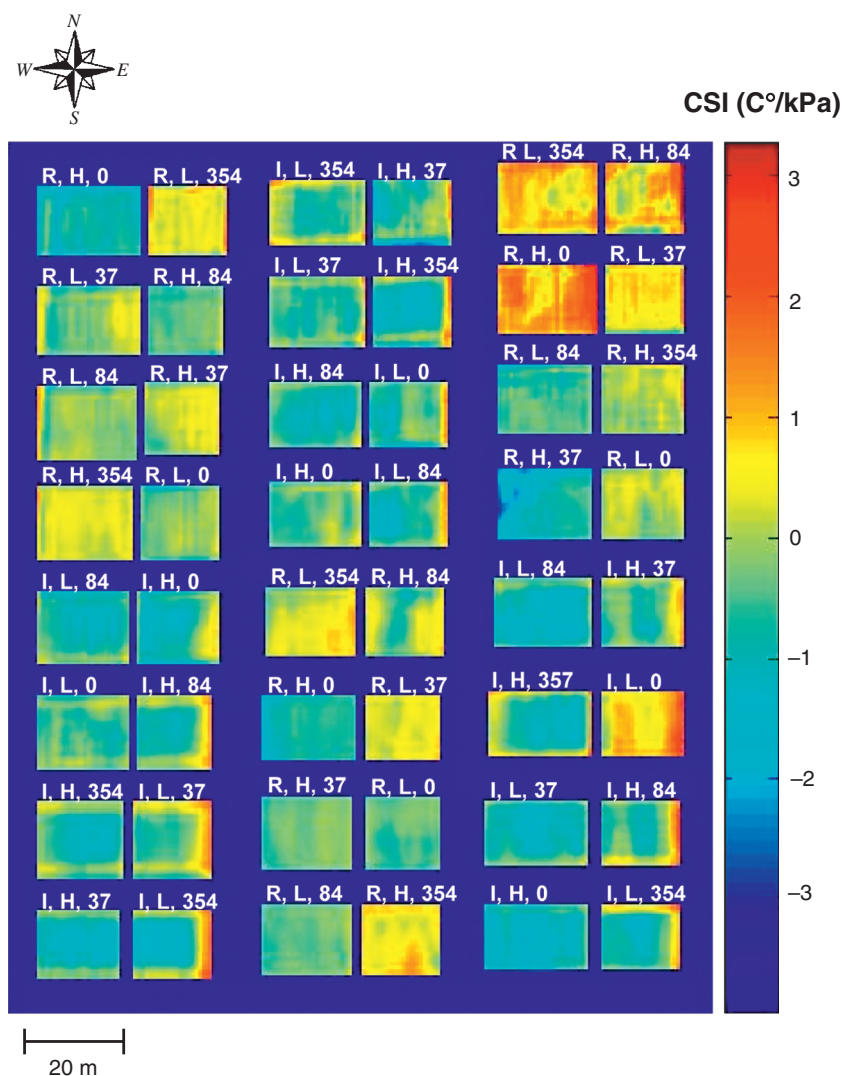


Fig. 9. Canopy stress index (CSI, C°/kPa) of the experimental field derived from a digital aerial thermal image taken on the 10 October 2004 at noon. R and I indicate rainfed and irrigated plots, H and L high and low plant densities, and 0, 16, 39, and 163 are kg N/ha. See the text for the derivation of the CSI.

first 3 days after anthesis, and that short-but-early extreme heat stresses can reduce grain growth to a greater extent than much longer periods of moderately high temperatures (Stone *et al.* 1995). In our experiment, the environmental conditions around anthesis were extreme enough (Fig. 3) to produce up to 60% of ear tipping in the rainfed, high-nitrogen treatment (Table 3). Ear tipping has been described in Australia (Fischer and Wood 1979), and is a trait commonly included in the screening for drought tolerance in wheat breeding programs. Drought during ear emergence often causes ear tipping.

The use of canopy temperature to quantify water stress in plants is based upon the assumption that as water becomes limiting, transpiration is reduced and plant temperature increases (Jackson *et al.* 1988). Canopy temperature is related

to the water status of the crop, net radiation, vapour pressure deficit, and wind speed. In the main cereal-growing regions of western Victoria, spatial variability in the water status of field crops is usually caused by spatial patterns of subsoil constraints such as salinity, sodicity, soil strength (Sadras *et al.* 2003; Rodriguez *et al.* 2005), or root pests and diseases. These conditions can lead to changes in canopy transpiration as a result of active regulation of stomata aperture (Pinter *et al.* 1979; Nilsson 1995). These spatial changes in canopy temperature can be instantly and remotely recorded by thermographic imaging (Fig. 1). Inoue (1990) showed that thermal imaging of a crop canopy could reveal the spatial differences in canopy surface temperatures and suggested that differences in the physiological status of the plants could be easily detected using this technology.

The technology has clear advantages over point-based IR thermometry, to reveal spatial patterns in the field (Chaerle and van der Straten 2000). Furthermore, from the combination of micrometeorological data and digital thermal images, spatial patterns for canopy conductance, canopy transpiration, and irrigation requirements could be derived (Inoue and Moran 1997).

One of the main drawbacks of the technology is that thermal images are complex combinations of crop and soil thermal emissions. Particularly before full ground cover, important differences between the actual crop temperature and the sensed canopy temperature exist (Wanjura *et al.* 2004). A method to retrieve useful information from thermal images of potted plants was developed by Leinonen and Jones (2004). Their method requires the overlaying of thermal and visible images, and a classification procedure using sophisticated imaging software. In our work we devised a simpler alternative to retrieve the temperature of the crop from digital thermal images and ground cover measurement of wheat canopies. This was based on the fact that absorbed PAR has been well related to spectral reflectance measurements (Gallo *et al.* 1985; Inoue and Iwasaki 1991), and that the relationship between the fractional intercepted PAR and spectral indices derived from reflectance measurements is little affected by solar zenith angle or time of the day (Pinter 1993). These results suggest that the use of multi-spectral vegetation indices to estimate $1 - f$ and ground cover is biophysically sound (Inoue and Moran 1997).

We showed that by normalising the canopy temperature depression using VPD, the resulting CSI was able to capture physiological responses at both the leaf and crop levels. At leaf level, CSI explained a significant proportion of the variation in net photosynthesis, stomatal conductance, and transpiration rate (Fig. 5). The observed changes in these physiological variables indicate that both photosynthesis and transpiration were primarily regulated by stomatal behaviour, although they are also affected by VPD, and the resistance for carboxylation (Lawlor 1993).

At the crop level, CSI was related to both shoot growth rate before anthesis and grain yield. Environmental variation in wheat yield is known to be greatly driven by changes in the number of kernels per unit area (Fischer 1980), through effects on the rate of crop growth around anthesis (Fischer 1980; Robertson and Giunta 1994). In Fig. 7 we show that the rate of crop growth around anthesis was highly related to grain yield, and that the slope of the relationship was similar to that derived from the dataset in Robertson and Giunta (1994). We believe that this supports our argument that CSI is a meaningful variable capable of describing the physiological status of the crop at anthesis, as CSI was not only linearly related to the final grain yield, but also to the growth rate around anthesis. Relationships between canopy temperature depression and grain yield have been reported

previously. For wheat, Amani *et al.* (1996) found a 17% yield change per degree of change in the difference between canopy and air temperatures in a hot, dry environment of Mexico. In wheat and cotton, high-yielding cultivars are better able to maintain lower canopy temperatures (Radin 1994; Amani *et al.* 1996). It is important to notice that canopy temperature alone, particularly if it is not instantly determined from a thermal image of the whole area under study, cannot be used as an absolute estimator of the physiological status of the crop. This is because leaf temperature depends on its energy budget resulting from incoming solar radiation, outgoing long-wave radiation, and latent and sensitive heat fluxes, which are affected by rapidly changing micrometeorological conditions (Dunin *et al.* 1991). Therefore, spatial temperature information becomes meaningful when adjusted by micrometeorological conditions, or incorporated into a stress index (Inoue 1990).

We do not expect CSI to account for yield responses to extreme conditions, e.g. heat stress or frost around anthesis. However, despite the extreme environmental conditions around anthesis in this experiment, CSI explained important physiological processes and variables at both leaf and canopy levels. CSI also provides a simple and elegant link with crop models to spatially simulate key physiological traits of wheat canopies, i.e. 'spatialise' crop models. This is the application of a crop model over areas larger than that for which it has been originally developed (Favre *et al.* 2004). This might require more refined models (Rodriguez *et al.* 2001) able to relate existing remotely sensed information to the unavailable data, i.e. spatial variations in soil properties, landscape properties, and crop condition, needed for the model to produce outputs and correct model calculations at larger scales than the point.

Conclusions

In this work we developed a method to extract valuable crop temperature information from complex digital thermal images of crop canopies, and proposed a canopy stress index that can be applied at spatial scales, commensurate with the needs of site-specific management and variable rate technologies of precision agriculture. This index was capable of describing physiological processes and variables at both the leaf and canopy levels to describe the physiological status of crops.

Acknowledgments

This work was fully funded by the Department of Primary Industries of Victoria, Australia. The collaboration with Victor Sadras was funded by GRDC (project CS0212). J. Angus provided valuable comments on this manuscript. We greatly appreciate and commend the excellent technical work provided by Russel Argall.

References

- Amani I, Fischer RA, Reynolds MP (1996) Canopy temperature depression association with yield of irrigated spring wheat cultivars in a hot climate. *Journal Agronomy and Crop Science* **176**, 119–129.
- Barnes EM, Clarke TR, Richards SE (2000) Coincident detection of crop water stress, nitrogen status and canopy density using ground based Multispectral data. In 'Proceedings of the 5th International Conference on Precision Agriculture'. (ASA-CSSA-SSSA: Bloomington, MN)
- Blackmer TM, Schepers JS, Varvel GE, Walter-Shea EA (1996) Nitrogen deficiency detection of reflected short-wave radiation from irrigated corn canopies. *Agronomy Journal* **88**, 1–5.
- Boccardo M, Boue C, Garmier M, de Paepe R, Boccardo AC (2001) Infra-red thermography revealed a role for mitochondria in pre-symptomatic cooling during harpin-induced hypersensitive response. *The Plant Journal* **28**, 663–670. doi: 10.1046/j.1365-313x.2001.01186.x
- Bowden RL, Rouse DI, Sharkey TD (1990) Mechanism of photosynthesis decrease by *Verticillium dahliae* in potato. *Plant Physiology* **94**, 1048–1055.
- Bringham IJ (2001) Soil-root-canopy interactions. *Annals of Applied Biology* **138**, 243–251.
- Broadley MR, Escobar-Gutierrez AJ, Burns A, Burns IG (2001) Nitrogen limited growth of lettuce is associated with lower stomatal conductance. *New Phytologist* **152**, 97–106. doi: 10.1046/j.0028-646x.2001.00240.x
- Chaerle L, van Caeneghem W, Messens E, Lambers H, van Montagu M, van der Straeten D (1999) Presymptomatic visualization of plant-virus interactions by thermography. *Nature Biotechnology* **17**, 813–816. doi: 10.1038/11765
- Chaerle L, van der Straeten D (2000) Imaging techniques and early detection of plant stress. *Trends in Plant Science* **5**, 495–501. doi: 10.1016/S1360-1385(00)01781-7
- Clarke TR (1997) An empirical approach for detecting water stress using multispectral airborne sensors. *HortTechnology* **7**, 9–16.
- Dunin FX, Barrs HD, Meyer WS, Trevitt ACF (1991) Foliage temperature and latent heat flux of irrigated wheat. *Agricultural and Forest Meteorology* **55**, 133–147. doi: 10.1016/0168-1923(91)90027-N
- Faivre R, Leenhardt D, Voltz M, Benoit M, Papy F, Dedieu G, Wallach D (2004) Spatialising crop models. *Agronomie* **24**, 205–217. doi: 10.1051/agro:2004016
- Filella J, Peñuelas J (1994) The red-edge position and shift as indicators of plant chlorophyll content, biomass and hydric status. *International Journal of Remote Sensing* **15**, 1459–1470.
- Fischer RA (1980) Influence of water stress on crop yield in semiarid regions. In 'Adaptation of plants to water and high temperature stress'. (Eds NC Turner, PJ Kramer) pp. 323–339. (Wiley: New York)
- Fischer RA (1985) Number of kernels in wheat crops and the influence of solar radiation and temperature. *Journal of Agricultural Science* **105**, 447–461.
- Fischer RA, Wood JT (1979) Drought resistance in spring wheat cultivars. III. Yield associations with morpho-physiological traits. *Australian Journal of Agricultural Research* **30**, 1001–1020. doi: 10.1071/AR9791001
- Gallo KP, Daughtry CST, Bauer ME (1985) Spectral estimates of absorbed photosynthetically active radiation in corn canopies. *Remote Sensing of Environment* **17**, 221–232. doi: 10.1016/0034-4257(85)90096-3
- Garrity DP, O'Toole JC (1995) Selection for reproductive stress drought avoidance in rice, using infrared thermometry. *Agronomy Journal* **87**, 773–779.
- van Herwaarden AF, Angus JF, Richards RA, Farquhar GD, Howe GN (1998a) 'Haying-off', the negative grain yield response of dryland wheat to nitrogen fertiliser. I. Biomass, grain yield, and water use. *Australian Journal of Agricultural Research* **51**, 147–154.
- van Herwaarden AF, Farquhar GD, Angus JF, Richards RA, Howe GN (1998b) 'Haying-off', the negative grain yield response of dryland wheat to nitrogen fertilizer. II. Carbohydrates and protein dynamics. *Australian Journal of Agricultural Research* **49**, 1083–1094. doi: 10.1071/A97040
- Huete AR (1988) A soil-adjusted vegetation index (SAVI). *Remote Sensing of Environment* **25**, 295–309. doi: 10.1016/0034-4257(88)90106-X
- Idso S (1982) Non-water-stress baselines: a key to measuring and interpreting plant water stress. *Agricultural and Forest Meteorology* **27**, 59–70.
- Idso SB, Jackson RD, Pinter PJ Jr, Moran MS, Reginato RJ, Hartfield JL (1981) Normalising the stress-degree-day parameter for environmental variability. *Agricultural and Forest Meteorology* **24**, 45–55.
- Inoue Y (1990) Remote detection of physiological depression in crop plants with infrared thermal imagery. *Nihon Sakumotsu Gakkai Kiji* **59**, 762–768.
- Inoue Y, Iwasaki K (1991) Spectral estimation of radiation absorptance and leaf area index in corn canopies as affected by canopy architecture and growth stage. *Nihon Sakumotsu Gakkai Kiji* **60**, 578–580.
- Inoue Y, Moran MS (1997) A simplified method for remote sensing of daily canopy transpiration. A case study with direct measurements of canopy transpiration in soybean canopies. *International Journal of Remote Sensing* **17**, 139–152.
- Jackson RD (1982) Canopy temperature and crop water stress. In 'Advances in irrigation'. (Ed. D Hillel) pp. 43. (Academic Press: New York)
- Jackson RD, Hatfield JL, Reginato RJ, Idso SB, Pinter PJ Jr (1983) Estimation of daily evapotranspiration from one time-of-day measurements. *Agricultural Water Management* **7**, 351–362. doi: 10.1016/0378-3774(83)90095-1
- Jackson RD, Idso SB, Reginato RJ, Pinter PJ Jr (1981) Canopy temperature as a crop water stress indicator. *Water Resources Research* **17**, 1133–1138.
- Jackson RD, Kustas WP, Choudhury BJ (1988) A re-examination of the crop water stress index. *Irrigation Science* **9**, 309–317. doi: 10.1007/BF00296705
- Jones HDH, Corlett JE, Massacci A (1995) Drought enhances stomatal closure in response to shading in sorghum (*Sorghum bicolor*) and in millet (*Pennisetum americanum*). *Australian Journal of Plant Physiology* **22**, 1–6.
- Jordan CF (1979) Derivation of leaf area index from quality of light on the forest floor. *Ecology* **50**, 663–666.
- Lawlor DW (1993) 'Photosynthesis: molecular, physiological, and environmental processes.' p. 318. (Longman Scientific and Technical: Essex, UK)
- Leinonen I, Jones HG (2004) Combining thermal and visible imagery for estimating canopy temperature and identifying plant stress. *Journal of Experimental Botany* **55**, 1423–1431. doi: 10.1093/jxb/erh146
- Loomis RS, Connor DJ (1996) 'Crop ecology. Productivity and management in agricultural systems.' (Cambridge University Press: Cambridge, UK)
- Moran MS, Clarke TR, Inoue Y, Vidal A (1994) Estimating crop water deficit using the relation between surface-air temperature and spectral vegetation index. *Remote Sensing of Environment* **49**, 246–263. doi: 10.1016/0034-4257(94)90020-5

- Moran MS, Inoue Y, Barnes EM (1997) Opportunities and limitations for image-based remote sensing in precision crop management. *Remote Sensing of Environment* **61**, 319–346. doi: 10.1016/S0034-4257(97)00045-X
- Nilsson HE (1995) Remote sensing and image analysis in plant pathology. *Annual Review of Phytopathology* **33**, 489–527. doi: 10.1146/annurev.py.33.090195.002421
- Peñuelas J, Filella J (1998) Visible and near-infrared reflectance techniques for diagnosing plant physiological status. *Trends in Plant Science* **3**, 151–156. doi: 10.1016/S1360-1385(98)01213-8
- Pinter PJ Jr (1993) Solar angle independence in the relationship between absorbed PAR and remotely sensed data for alfalfa. *Remote Sensing of Environment* **46**, 19–25. doi: 10.1016/0034-4257(93)90029-W
- Pinter PJ Jr, Stanghellini ME, Reginato RJ, Jenkins AD, Jackson RD (1979) Remote detection of biological stresses in plants with infrared thermometry. *Science* **205**, 585–587.
- Price JC, Bausch WC (1995) Leaf area index estimation from visible and near-infrared reflectance data. *Remote Sensing of Environment* **52**, 55–65. doi: 10.1016/0034-4257(94)00111-Y
- Radin JW (1994) Genetic variability for stomatal conductance in Pima cotton and its relation to improvements of heat adaptation. *Proceedings of the National Academy of Sciences of the United States of America* **91**, 7217–7221.
- Radin JW, Mauney JR, Guinn G (1985) Effects of N fertility on plant water relations and stomatal responses to water stress in irrigated cotton. *Crop Science* **25**, 110–115.
- Railyan V, Korobov RM (1993) Red edge structure of canopy reflectance spectra of Triticale. *Remote Sensing of Environment* **46**, 173–182. doi: 10.1016/0034-4257(93)90093-D
- Robertson MJ, Giunta F (1994) Response of spring wheat exposed to pre-anthesis water stress. *Australian Journal of Agricultural Research* **45**, 19–35. doi: 10.1071/AR9940019
- Rodriguez D, Ewert F, Goudriaan J, Manderscheid R, Burkart S, Weigel HJ (2001) Modelling the response of wheat canopy assimilation to atmospheric CO₂ concentrations. *New Phytologist* **150**, 337–346. doi: 10.1046/j.1469-8137.2001.00106.x
- Rodriguez D, Nuttall J, Sadras V, Rees van H, Armstrong RD (2005) Impact of subsoil constraints on wheat yield and gross margin on fine-textured soils of the southern Victorian Mallee. *Australian Journal of Agricultural Research* (In press).
- Rouse JW, Haas RH, Schell JA, Deering DW (1973) Monitoring vegetation systems in the great plains with ERTS. In 'Proceedings of the 3rd ERTS Symposium, NASA SP-351'. Vol. 1, pp. 309–317. (NASA: Washington, DC)
- Russell G, Wilson GW (1994) 'An agri-pedo-climatological knowledge-base of wheat in Europe.' p. 158. (Joint Research Centre, European Commission: Luxembourg)
- Sadras VO, Baldock J, Cox J, Bellotti B (2004) Crop rotation effect on wheat grain yield as mediated by changes in the degree of water and nitrogen co-limitation. *Australian Journal of Agricultural Research* **55**, 599–607. doi: 10.1071/AR04012
- Sadras VO, Baldock J, Roget D, Rodriguez D (2003) Measuring and modelling yield and water budget components of wheat crops in coarse-textured soils with chemical constraints. *Field Crops Research* **84**, 241–260. doi: 10.1016/S0378-4290(03)00093-5
- Sadras VO, Wilson LJ (1997) Growth analysis of cotton crops infested with spider-mites. I. Light interception and radiation-use efficiency. *Crop Science* **37**, 481–491.
- Stone PJ, Nicolas ME (1995) Effect of timing of heat stress during grain-filling on two wheat varieties differing in heat tolerance. I. Grain growth. *Australian Journal of Plant Physiology* **22**, 927–934.
- Stone PJ, Savin R, Wardlaw IF, Nicolas ME (1995) The influence of recovery temperature on the effects of a brief heat shock on wheat. I. Grain growth. *Australian Journal of Plant Physiology* **22**, 945–954.
- Stone ML, Solie JB, Raun WR, Whitney RW, Taylor SL, Ringer JD (1997) Use of spectral radiance for correcting in-season fertiliser nitrogen deficiencies in winter wheat. *Transactions of the American Society of Agricultural Engineers* **39**, 1623–1631.
- Wanjura DF, Maas SJ, Winslow JC, Upchurch DR (2004) Scanned and spot measured canopy temperatures of cotton and corn. *Computers and Electronics in Agriculture* **44**, 33–48. doi: 10.1016/j.compag.2004.02.005
- Wheeler TR, Hong TD, Ellis RH, Batts GR, Morison JIL, Hadley P (1996) The duration and rate of grain growth, and harvest index, of wheat (*Triticum aestivum* L.) in response to temperature and CO₂. *Journal of Experimental Botany* **47**, 623–630.

Manuscript received 10 February 2005, accepted 23 June 2005